Mechanistic Analysis of the Unusual Redox-Elimination Sequence Employed by *Thermotoga maritima* BglT: A 6-Phospho-β-glucosidase from Glycoside Hydrolase Family 4[†]

Vivian L. Y. Yip and Stephen G. Withers*

2036 Main Mall, Department of Chemistry, University of British Columbia, Vancouver, British Columbia, Canada V6T 1Z1

Received October 9, 2005; Revised Manuscript Received November 8, 2005

ABSTRACT: "Classical" glycosidases utilize either direct or double-displacement mechanisms involving oxocarbenium ion-like transition states to catalyze the hydrolysis of glycosidic bonds. By contrast, the mechanism of the glycosidases in glycoside hydrolase family 4 has been recently proposed to involve NAD^+-mediated redox steps along with α,β-elimination and addition steps via anionic intermediates. Support for this mechanism in BglT, a 6-phospho-β-glucosidase in family 4, has been provided through mechanistic and X-ray crystallographic analyses [Yip, V. L.Y., et al. (2004) *J. Am. Chem. Soc. 126*, 8354−8355] in which primary deuterium kinetic isotope effects for the hydride abstraction at C3 and for the α-proton abstraction at C2 indicate that these two steps are both partially rate-limiting. Current data reveal that there is no secondary deuterium kinetic isotope effect associated with the rehybridization of the C1 sp^3 center to a sp^2 center. Furthermore, a flat linear free energy relationship was established with a series of aryl 6-phospho-β-D-glucosides of varying leaving group abilities. Taken together, these data indicate that cleavage of the C1−O1 linkage does not occur during a rate-limiting step. Since the deprotonation at C2 is slow and partially rate-limiting while the departure of the leaving group is not, a stepwise $E1_{cb}$-type mechanism rather than an E1 or a concerted E2-syn mechanism is proposed. Direct evidence for the role of NAD^+ was obtained by reduction in situ using $NaBH_4$ leading to an inactive enzyme that could be reactivated by the addition of excess NAD^+. This was accompanied by the expected UV−vis spectrophotometric changes.

Glycosidases, transglycosidases, glycosyltransferases, polysaccharide lyases, and carbohydrate esterases are classes of enzymes included in the CAZY (carbohydrate-active enzyme) database (http://afmb.cnrs-mrs.fr/~cazy/CAZY/index.html) (*1*, *2*). For each class of enzymes, the CAZY database organizes enzymes into different families based on primary sequence similarity, which is in turn a reliable predictor of structure as well as mechanism (*3*). There are currently close to 100 families of glycosidases, and all, with the exception of the members of family 4 (*4*−*6*), catalyze hydrolysis of the glycosidic bond through either a direct displacement or a double-displacement mechanism via oxocarbenium ion-like transition states (*7*−*10*), as first proposed by Koshland in 1953 (*11*).

Glycoside hydrolase family 4 (GH4)[1] members all derive from bacterial sources and require two cofactors, NAD^+ and a divalent metal (Mn^{2+}, Ni^{2+}, Co^{2+}, Mg^{2+}, or Ca^{2+}) for activity (*4*−*6*, *12*−*17*). In some cases, reducing conditions are also required (*5*, *12*−*17*). Furthermore, while all other glycosidase families contain only enzymes that catalyze the hydrolysis of substrates with the same anomeric configuration,[2] GH4 includes both α- and β-glycosidases (*5*, *6*, *12*, *14*−*20*). This highly unusual requirement for NAD^+ and the seemingly loose specificity for the substrate anomeric configuration have spurred interest in the mechanism of GH4 enzymes. Recent mechanistic and structural data on two GH4 members, BglT (*5*, *6*) from *Thermotoga maritima* and GlvA

[†] This work was supported by grants from the Natural Sciences and Engineering Research Council of Canada, the Protein Engineering Network of Centres of Excellence, and the Canadian Institutes of Health Research. V.L.Y.Y. is funded by the Natural Sciences and Engineering Research Council of Canada and the Michael Smith Foundation for Health Research.

* To whom correspondence should be addressed. Telephone: (604) 822-3402. Fax: (604) 822-8869. E-mail: withers@chem.ubc.ca.

[1] Abbreviations: GH4, glycoside hydrolase family 4; NAD^+, β-nicotinamide adenine dinucleotide; NADH, β-nicotinamide adenine dinucleotide, reduced; $NADP^+$, β-nicotinamide adenine dinucleotide phosphate; NADPH, β-nicotinamide adenine dinucleotide phosphate, reduced; C6′P, cellobiose 6′-phosphate; 1[^{2}H]4NPG6P, 4-nitrophenyl 1-[^{2}H]-6-phospho-β-D-glucoside; 2[^{2}H]4NPG6P, 4-nitrophenyl 2-[^{2}H]-6-phospho-β-D-glucoside; 3[^{2}H]4NPG6P, 4-nitrophenyl 3-[^{2}H]-6-phospho-β-D-glucoside; 4NPG6P, 4-nitrophenyl 6-phospho-β-D-glucoside; 24DNPG6P, 2,4-dinitrophenyl 6-phospho-β-D-glucoside; 25DNPG6P, 2,5-dinitrophenyl 6-phospho-β-D-glucoside; 34DNPG6P, 3,4-dinitrophenyl 6-phospho-β-D-glucoside; 4C2NPG6P, 4-chloro-2-nitrophenyl 6-phospho-β-D-glucoside; 2NPG6P, 2-nitrophenyl 6-phospho-β-D-glucoside; 35DCPG6P, 3,5-dichlorophenyl 6-phospho-β-D-glucoside; 3NPG6P, 3-nitrophenyl 6-phospho-β-D-glucoside; 4CNPG6P, 4-cyanophenyl 6-phospho-β-D-glucoside; PG6P, phenyl 6-phospho-β-D-glucoside; 4tBuPG6P, 4-*tert*-butylphenyl 6-phospho-β-D-glucoside; KIE, kinetic isotope effect; ESI-MS, electrospray ionization mass spectrometry; UV−vis, ultraviolet−visible; G6P, glucose 6-phosphate; G6PDH, glucose-6-phosphate dehydrogenase; NMWL, nominal molecular weight limit.

[2] Although glycosidases from family 39, which includes both α-L-iduronidases and β-D-xylosidases (*32*), also appear to be an exception to this rule, the anomeric configurations of the substrates are the same and the presence of α- and β-glycosidases in the same family arises due to the conventions of nomenclature of D- and L-sugars.

10.1021/bi052054x CCC: $33.50
Published on Web 12/17/2005

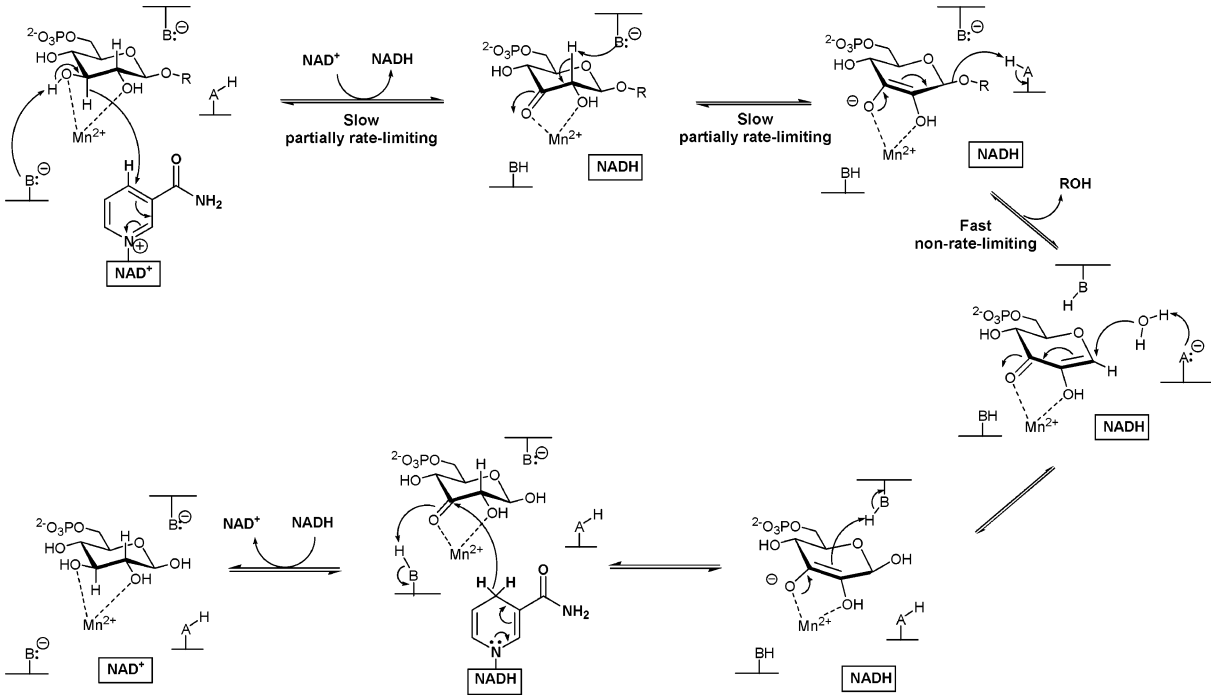

FIGURE 1: Proposed $E1_{cb}$ mechanism of BglT.

(*4*) from *Bacillus subtilis*, have led to a proposed mechanism that involves NAD^+-mediated redox steps as well as α,*β*-elimination of the glycosidic linkage (Figure 1) (*4*−*6*). This proposed mechanism is distinct from the two general glycosidase mechanisms, which for more than 50 years have served as incredibly reliable models for this class of enzymes.

Both BglT (6-phospho-*β*-glucosidase) and GlvA (6-phospho-α-glucosidase) were found to be retaining glycosidases (*4*−*6*). However, exchange of the C2 proton of the substrate with solvent deuterium during the enzymatic reaction revealed that cleavage of the C2−H2 bond occurs during the enzymatic reaction, which is inconsistent with either the direct or the double-displacement mechanisms (*4*−*11*). Furthermore, X-ray crystallographic data show that in BglT and GlvA the NAD^+ cofactor is 3.56 and 4.16 Å, respectively, from C3 of the glucose 6-phosphate (G6P) product (*4*−*6*). On the basis of these observations and mechanistic precedent from some dehydratases (*21*, *22*) and decarboxylases (*23*), it was proposed that both BglT and GlvA utilize the NAD^+ cofactor to oxidize the C3 hydroxyl of the substrate to a ketone, thereby activating the C2 proton for deprotonation, possibly by a tyrosine residue as the catalytic base (*4*−*6*). The enediolate intermediate thus formed is presumably stabilized by the Mn^{2+} cofactor, which is chelated to the C2 and C3 oxygen atoms (*4*−*6*). Subsequently, the C1−O1 linkage is cleaved via an α,*β*-elimination mechanism to generate an enzyme-bound α,*β*-unsaturated ketone intermediate. Water then adds to C1 via a 1,4-Michael-like addition, and the bound NADH reduces the 3-keto intermediate to give the final hydrolysis product. Preliminary evidence for the redox and elimination steps has been obtained from the small primary deuterium kinetic isotope effects (KIEs) measured for 4-nitrophenyl 2-[^{2}H]-6-phospho-*β*-D-glucoside (2[^{2}H]4NPG6P) and 4-nitrophenyl 3-[^{2}H]-6-phospho-*β*-D-glucoside (3[^{2}H]4NPG6P), implying that cleavage of the C2−H2 linkage and cleavage of the C3−H3 linkage represent (partially) rate-limiting steps (*5*). The following report expands upon the preliminary mechanistic analysis, providing further support for the proposed mechanism and more detailed insight.

MATERIALS AND METHODS

General Methods

All NMR spectra were recorded on Bruker Avance 300 and Bruker Avance 400 spectrometers at 300 and 400 MHz, respectively. Chemical shifts are reported on the *δ* scale in parts per million from tetramethylsilane (TMS) and were referenced to D_2O. ^{31}P NMR signals were externally referenced to 85% H_3PO_4 in H_2O at 0 ppm. Low- and high-resolution mass spectra were collected by the mass spectrometry laboratory at the University of British Columbia. Elemental analysis was performed by M. Lakha of the microanalysis laboratory at the University of British Columbia.

Materials

All chemicals and reagents were purchased from Sigma-Aldrich unless stated otherwise. The kinase BglK was donated by J. Thompson (*24*). All solvents were freshly distilled except where mentioned. Column chromatography was performed on 230−400 mesh silica gel.

Synthesis of Aryl Glucosides

All aryl *β*-D-glucosides were synthesized from 1,2,3,4,6-penta-*O*-acetyl-D-glucopyranose via the Koenigs−Knorr reaction (*25*). Aryl *β*-D-glucosides with leaving group phenols having pK_a values below 6 were deprotected with HCl in methanol (*26*). All other aryl *β*-D-glucosides were deprotected using sodium methoxide in methanol (*27*). 4-Nitrophenyl 1-[^{2}H]-*β*-D-glucoside was synthesized from 1-[^{2}H]-D-glucopyranose (purchased from Cambridge Isotope Laboratories, Inc.) via the Koenigs−Knorr reaction (*25*). Phosphorylation

of all compounds was accomplished enzymatically with BglK and adenosine 5′-triphosphate as described by Thompson and co-workers (*24*) with minor modifications. 4-Nitrophenyl 6-phospho-β-D-glucoside (4NPG6P) was prepared previously as described by Yip et al. (*5*). Characterization of all products is provided below.

4-Nitrophenyl 1-[^{2}H]-6-phospho-β-D-glucoside (1[^{2}H]-4NPG6P): ^{1}H NMR (400 MHz, D_2O) δ 8.05 (2 H, d, $J_{Ar2,Ar3} = J_{Ar5,Ar6} = 9.3$ Hz, Ar3, Ar5), 7.06 (2 H, d, $J_{Ar2,Ar3} = J_{Ar5,Ar6} = 9.3$ Hz, Ar2, Ar6), 3.98−3.93 (1 H, m, $H6_a$), 3.88−3.84 (1 H, m, $H6_b$), 3.59−3.49 (4 H, m, H2, H3, H4, H5); ^{13}C NMR (100 MHz, D_2O) δ 161.67 (C), 142.29 (C), 126.12 (2 CH), 116.40 (2 CH), 99.18 (1 C, $J_{1,D} = 23.4$ Hz, C1), 75.68 (d, $J_{5,P} = 6.5$ Hz, C5), 74.58 (C3), 72.78 (C2), 68.46 (C4), 62.54 (1 C, d, $J_{6,P} = 3.9$ Hz, C6); ^{31}P NMR (162 MHz, D_2O) δ 5.41 (1 P, t, $J_{H6,P} = 6.1$ Hz); ESI-MS *m/z* calcd for $[C_{12}H_{14}DNO_{11}PNa_2]^+$ 427.0241, found 427.0245. Anal. Calcd for $C_{12}H_{13}DNNa_2O_{11}P·2.5H_2O$: C, 30.57; H, 4.03; N, 2.97. Found: C, 31.40; H, 4.55; N, 3.36.

2,4-Dinitrophenyl 6-phospho-β-D-glucoside (24DNPG-6P): ^{1}H NMR (400 MHz, D_2O) δ 8.70 (1 H, d, $J_{Ar3,Ar5} = 2.8$ Hz, Ar3), 8.37 (1 H, dd, $J_{Ar5,Ar6} = 9.4$ Hz, $J_{Ar3,Ar5} = 2.8$ Hz, Ar5), 7.49 (1 H, d, $J_{Ar5,Ar6} = 9.4$ Hz, Ar6), 5.26 (1 H, d, $J_{1,2} = 7.6$ Hz, H1), 3.96−3.84 (2 H, m, $H6_a$, $H6_b$), 3.63−3.47 (4 H, m, H2, H3, H4, H5); ^{13}C NMR (100 MHz, D_2O) δ 154.23 (C), 141.30 (C), 138.62 (C), 129.86 (CH), 122.03 (CH), 117.59 (CH), 100.14 (C1), 76.02 (1 C, d, $J_{5,P} = 6.5$ Hz, C5), 74.63, 72.59, 68.26, 62.13 (1 C, d, $J_{6,P} = 4.3$ Hz, C6); ^{31}P NMR (162 MHz, D_2O) δ 4.88 (1 P, t, $J_{H6,P} = 5.9$ Hz); ESI-MS *m/z* calcd for $[C_{12}H_{14}N_2O_{13}PNa_2]^+$ 471.0029, found 471.0028. Anal. Calcd for $C_{12}H_{13}N_2O_{13}PNa_2·0.5H_2O$: C, 30.08; H, 2.94; N, 5.85. Found: C, 30.25; H, 3.19; N, 6.15.

2,5-Dinitrophenyl 6-phospho-β-D-glucoside (25DNPG-6P): ^{1}H NMR (400 MHz, D_2O) δ 8.06 (1 H, d, $J_{Ar4,Ar6} = 1.7$ Hz, Ar6), 7.97−7.92 (2 H, m, Ar3, Ar4), 5.25 (1 H, d, $J_{1,2} = 7.3$ Hz, H1), 3.99−3.94 (1 H, m, $H6_a$), 3.86−3.81 (1 H, m, $H6_b$), 3.65−3.46 (4 H, m, H2, H3, H4, H5); ^{13}C NMR (100 MHz, D_2O) δ 150.28 (C), 149.39 (C), 143.34 (C), 126.50 (CH), 117.87 (CH), 112.65 (CH), 100.34 (C1), 75.93 (1 C, d, $J_{5,P} = 7.0$ Hz, C5), 74.50, 72.67, 68.03, 61.99 (1 C, d, $J_{6,P} = 4.5$ Hz, C6); ^{31}P NMR (162 MHz, D_2O) δ 5.04 (1 P, t, $J_{H6,P} = 7.4$ Hz); ESI-MS *m/z* calcd for $[C_{12}H_{14}N_2O_{13}PNa_2]^+$ 471.0029, found 471.0030. Anal. Calcd for $C_{12}H_{13}N_2O_{13}PNa_2·H_2O$: C, 29.52; H, 3.10; N, 5.74. Found: C, 29.35; H, 3.39; N, 5.82.

3,4-Dinitrophenyl 6-phospho-β-D-glucoside (34DNPG-6P): ^{1}H NMR (400 MHz, D_2O) δ 8.70 (1 H, d, $J_{Ar2,Ar5} = 2.8$ Hz, Ar2), 8.37 (1 H, dd, $J_{Ar5,Ar6} = 9.4$ Hz, $J_{Ar2,Ar5} = 2.8$ Hz, Ar5), 7.49 (1 H, d, $J_{Ar5,Ar6} = 9.4$ Hz, Ar6), 5.26 (1 H, d, $J_{1,2} = 7.6$ Hz, H1), 3.96−3.84 (2 H, m, $H6_a$, $H6_b$), 3.63−3.47 (4 H, m, H2, H3, H4, H5); ^{13}C NMR (100 MHz, D_2O) δ 154.23 (C), 141.30 (C), 138.62 (C), 129.86 (CH), 122.03 (CH), 117.59 (CH), 100.14 (C1), 76.02 (1 C, d, $J_{5,P} = 6.5$ Hz, C5), 74.63, 72.59, 68.26, 62.13 (1 C, d, $J_{6,P} = 4.3$ Hz, C6); ^{31}P NMR (162 MHz, D_2O) δ 4.88 (1 P, t, $J_{H6,P} = 5.9$ Hz); ESI-MS *m/z* calcd for $[C_{12}H_{14}N_2O_{13}PNa_2]^+$ 471.0029, found 471.0028. Anal. Calcd for $C_{12}H_{13}N_2O_{13}PNa_2·0.5H_2O$: C, 30.08; H, 2.94; N, 5.85. Found: C, 30.25; H, 3.19; N, 6.15.

4-Chloro-2-nitrophenyl 6-phospho-β-D-glucoside (4C2NPG-6P): ^{1}H NMR (400 MHz, D_2O) δ 7.86 (1 H, d, $J_{Ar3,Ar5} = 2.6$ Hz, Ar3), 7.53 (1 H, dd, $J_{Ar5,Ar6} = 9.1$ Hz, $J_{Ar3,Ar5} = 2.6$ Hz, Ar5), 7.30 (1 H, d, $J_{Ar5,Ar6} = 9.1$ Hz, Ar6), 5.08 (1 H, d, $J_{1,2} = 7.5$ Hz, H1), 3.94−3.88 (1 H, m, $H6_a$), 3.84 (1 H, ddd, $J = 12.2$ Hz, $J = 5.7$ Hz, $J = 1.5$ Hz, $H6_b$), 3.59−3.43 (4 H, m, H2, H3, H4, H5); ^{13}C NMR (75 MHz, D_2O) δ 149.81 (C), 141.27 (C), 136.35 (CH), 128.76 (C), 126.84 (CH), 120.45 (CH), 102.16 (C1), 77.39 (1 C, d, $J_{5,P} = 6.8$ Hz, C5), 76.27, 74.27, 69.91, 63.73 (1 C, d, $J_{6,P} = 4.1$ Hz, C6); ^{31}P NMR (162 MHz, D_2O) δ 5.03 (1 P, t, $J_{H6,P} = 8.1$ Hz); ESI-MS *m/z* calcd for $[C_{12}H_{14}ClNNa_2O_{11}P]^+$ 459.9788, found 459.9786. Anal. Calcd for $C_{12}H_{13}ClNNa_2O_{11}P·2.5H_2O$: C, 28.53; H, 3.57; N, 2.77. Found: C, 28.94; H, 3.96; N, 3.00.

2-Nitrophenyl 6-phospho-β-D-glucoside (2NPG6P): ^{1}H NMR (400 MHz, D_2O) δ 7.75 (1 H, dd, $J_{Ar3,Ar4} = 8.2$ Hz, $J_{Ar3,Ar5} = 1.5$ Hz, Ar3), 7.53−7.49 (1 H, m, Ar5), 7.28 (1 H, d, $J_{Ar5,Ar6} = 8.2$ Hz, Ar6), 7.07 (1 H, t, $J_{Ar3,Ar4} = J_{Ar4,Ar5} = 8.2$ Hz, Ar4), 5.09 (1 H, d, $J_{1,2} = 7.4$ Hz, H1), 3.96−3.90 (2 H, m, $H6_a$), 3.84 (1 H, ddd, $J = 12.2$ Hz, $J = 5.6$ Hz, $J = 1.3$ Hz, $H6_b$), 3.60−3.45 (4 H, m, H2, H3, H4, H5); ^{13}C NMR (100 MHz, D_2O) δ 149.37 (C), 139.52 (C), 135.23 (CH), 125.55 (CH), 122.96 (CH), 117.24 (CH), 100.47 (C1), 75.81 (1 C, d, $J_{5,P} = 6.8$ Hz, C5), 74.71, 72.80, 68.36, 62.17 (1 C, d, $J_{6,P} = 3.8$ Hz, C6); ^{31}P NMR (162 MHz, D_2O) δ 5.17 (1 P, t, $J_{H6,P} = 6.2$ Hz); ESI-MS *m/z* calcd for $[C_{12}H_{15}NO_{11}PNa_2]^+$ 426.0178, found 426.0173. Anal. Calcd for $C_{12}H_{14}NNa_2O_{11}P·3H_2O$: C, 30.07; H, 4.21; N, 2.92. Found: C, 30.47; H, 4.38; N, 3.00.

3,5-Dichlorophenyl 6-phospho-β-D-glucoside (35DCPG-6P): ^{1}H NMR (400 MHz, D_2O) δ 7.05 (1 H, t, $J_{Ar2,Ar4} = J_{Ar4,Ar6} = 1.6$ Hz, Ar4), 6.96 (2 H, d, $J_{Ar2,Ar4} = J_{Ar4,Ar6} = 1.6$ Hz, Ar2, Ar6), 4.96 (1 H, d, $J_{1,2} = 7.6$ Hz, H1), 3.98−3.92 (1 H, m, $H6_a$), 3.82 (1 H, ddd, $J = 12.4$ Hz, $J = 5.6$ Hz, $J = 1.6$ Hz, $H6_b$), 3.62−3.41 (4 H, m, H2, H3, H4, H5); ^{13}C NMR (75 MHz, D_2O) δ 158.87 (C), 136.44 (CH), 124.53 (2 C), 116.89 (2 CH), 101.55 (C1), 77.19 (1 C, $J_{5,P} = 7.0$ Hz, C5), 76.12, 74.41, 69.79, 63.58 (1 C, $J_{6,P} = 3.2$ Hz, C6); ^{31}P NMR (162 MHz, D_2O) δ 5.03 (1 P, t, $J_{H6,P} = 5.7$ Hz); ESI-MS *m/z* calcd for $[C_{12}H_{14}O_9PNa_2Cl_2]^+$ 448.9548, found 448.9540. Anal. Calcd for $C_{12}H_{13}O_9PNa_2Cl_2·3H_2O$: C, 28.65; H, 3.81. Found: C, 28.83; H, 3.98.

3-Nitrophenyl 6-phospho-β-D-glucoside (3NPG6P): ^{1}H NMR (400 MHz, D_2O) δ 7.80 (1 H, ddd, $J_{Ar4,Ar5} = 8.3$ Hz, $J_{Ar2,Ar4} = 2.1$ Hz, $J_{Ar4,Ar6} = 1.3$ Hz, Ar4), 7.75 (1 H, t, $J_{Ar2,Ar4} = J_{Ar2,Ar6} = 2.1$ Hz, Ar2), 7.41 (1 H, t, $J_{Ar4,Ar5} = J_{Ar5,Ar6} = 8.3$ Hz, Ar5), 7.36 (1 H, ddd, $J_{Ar5,Ar6} = 8.3$ Hz, $J_{Ar2,Ar6} = 2.1$ Hz, $J_{Ar4,Ar6} = 1.3$ Hz, Ar6), 5.09−5.07 (1 H, m, H1), 3.97−3.92 (1 H, m, $H6_a$), 3.83 (1 H, ddd, $J = 12.3$ Hz, $J = 5.5$ Hz, $J = 1.6$ Hz, $H6_b$), 3.62−3.54 (2 H, m, H5, H3), 3.52−3.46 (2 H, m, H2, H4); ^{13}C NMR (100 MHz, D_2O) δ 156.71 (C), 148.55 (C), 130.59 (CH), 123.17 (CH), 117.94 (CH), 111.45 (CH), 100.06 (C1), 75.68 (1 C, d, $J_{5,P} = 6.9$ Hz, C5), 74.63, 72.92, 68.32, 62.08 (1 C, $J_{6,P} = 4.5$ Hz, C6); ^{31}P NMR (162 MHz, D_2O) δ 5.04 (1 P, t, $J_{H6,P} = 6.3$ Hz); ESI-MS *m/z* calcd for $[C_{12}H_{15}NO_{11}PNa_2]^+$ 426.0178, found 426.0175. Anal. Calcd for $C_{12}H_{14}NNa_2O_{11}P·3H_2O$: C, 30.07; H, 4.21; N, 2.92. Found: C, 30.47; H, 4.61; N, 2.77.

4-Cyanophenyl 6-phospho-β-D-glucoside (4CNPG6P): ^{1}H NMR (400 MHz, D_2O) δ 7.60 (2 H, d, $J_{Ar2,Ar3} = J_{Ar4,Ar5} = 7.5$ Hz, Ar3, Ar5), 7.09 (2 H, d, $J_{Ar2,Ar3} = J_{Ar4,Ar5} = 7.5$ Hz, Ar2, Ar6), 5.08−5.06 (1 H, m, H1), 3.95−3.84 (2 H, m, $H6_a$, $H6_b$), 3.56−3.47 (4 H, m, H2, H3, H4, H5); ^{13}C NMR

(100 MHz, D_2O) δ 159.94 (C), 134.51 (2 CH), 119.64 (C), 116.81 (2 CH), 104.88 (CN), 99.35 (C1), 75.58 (1 C, d, $J_{5,P}$ = 7.1 Hz, C5), 74.72, 72.80, 68.41, 62.28 (1 C, d, $J_{6,P}$ = 4.3 Hz, C6); ^{31}P NMR (162 MHz, D_2O) δ 4.28 (1 P, t, $J_{H6,P}$ = 5.2 Hz); ESI-MS *m/z* calcd for $[C_{13}H_{15}NO_9PNa_2]^+$ 406.0280, found 406.0279. Anal. Calcd for $C_{13}H_{14}NNa_2O_9P\cdot 2H_2O$: C, 35.38; H, 4.08; N, 3.17. Found: C, 35.72; H, 4.00; N, 3.16.

Phenyl 6-phospho-β-D-glucoside (PG6P): ^{1}H NMR (400 MHz, D_2O) δ 7.25−7.21 (2 H, m, Ar3, Ar5), 7.00−6.96 (3 H, m, Ar2, Ar4, Ar6), 4.97 (1 H, d, $J_{1,2}$ = 7.6 Hz, H1), 3.95−3.89 (1 H, m, $H6_a$), 3.82 (1 H, ddd, J = 12.4 Hz, J = 5.6 Hz, J = 1.6 Hz, $H6_b$), 3.59−3.41 (4 H, m, H2, H3, H4, H5); ^{13}C NMR (100 MHz, D_2O) δ 156.44 (C), 129.84 (2 CH), 123.18 (CH), 116.43 (2 CH), 100.19 (C1), 75.52 (1 C, d, $J_{5,P}$ = 6.9 Hz, C5), 74.82, 73.06, 68.51, 62.21 (1 C, d, $J_{6,P}$ = 4.3 Hz, C6); ^{31}P NMR (162 MHz, D_2O) δ 5.80 (1 P, t, $J_{H6,P}$ = 8.3 Hz); ESI-MS *m/z* calcd for $[C_{12}H_{16}O_9PNa_2]^+$ 381.0327, found 381.0325. Anal. Calcd for $C_{12}H_{15}Na_2O_9P\cdot 0.75H_2O$: C, 36.61; H, 4.22. Found: C, 37.19; H, 4.76.

4-tert-Butylphenyl 6-phospho-β-D-glucoside (4tBuPG-6P): ^{1}H NMR (400 MHz, D_2O) δ 7.31 (2 H, d, $J_{Ar2,Ar3}$ = $J_{Ar5,Ar6}$ = 8.6 Hz, Ar3, Ar5), 6.95 (2 H, d, $J_{Ar2,Ar3}$ = $J_{Ar5,Ar6}$ = 8.6 Hz, Ar2, Ar6), 4.93 (1 H, d, $J_{1,2}$ = 7.2 Hz, H1), 3.95−3.89 (1 H, m, $H6_a$), 3.87−3.83 (1 H, m, $H6_b$), 3.57−3.40 (4 H, m, H2, H3, H4, H5), 1.12 (9 H, s, 3 CH_3); ^{13}C NMR (100 MHz, D_2O) δ 154.30 (C), 146.56 (C), 126.65 (2 CH), 116.25 (2 CH), 100.49 (C1), 75.48 (1 C, d, $J_{5,P}$ = 6.9 Hz, C5), 74.90, 73.06, 68.60, 62.37 (1 C, d, $J_{6,P}$ = 4.4 Hz, C6), 33.50 (C), 30.51 (3 CH_3); ^{31}P NMR (121 MHz, D_2O) δ 4.24 (1 P, t, $J_{H6,P}$ = 5.7 Hz); ESI-MS *m/z* calcd for $[C_{16}H_{24}O_9PNa_2]^+$ 437.0953, found 437.0952. Anal. Calcd for $C_{16}H_{23}O_9PNa_2\cdot 2H_2O$: C, 40.69; H, 5.76. Found: C, 40.98; H, 6.04.

Cellobiose 6′-phosphate (C6′P): ^{1}H NMR (400 MHz, D_2O) δ 5.05 (1 H, d, $J_{\alpha1,\alpha2}$ = 3.7 Hz, αH1), 4.49 (1 H, d, $J_{\beta1,\beta2}$ = 8.0 Hz, βH1), 4.34 (1 H, d, $J_{1',2'}$ = 7.9 Hz, H1′), 3.85−3.64, 3.48−3.33, 3.19−3.11; ^{13}C NMR (100 MHz, D_2O) δ 102.73 (α,βC1′), 95.58 (βC1), 91.66 (αC1), 79.25, 79.13 (2 CH), 75.24 (1 C, d, $J_{5',P}$ = 6.9 Hz, C5′), 74.89 (3 CH), 74.63, 74.21, 73.68, 73.21 (2 CH), 71.23, 71.01, 69.95, 68.89, 68.86, 62.73 (1 C, d, $J_{6',P}$ = 3.8 Hz, C6′), 60.03, 59.87; ^{31}P NMR (162 MHz, D_2O) δ 4.91 (1 P, t, $J_{H6',P}$ = 5.7 Hz); ESI-MS *m/z* calcd for $[C_{12}H_{22}O_{14}PNa_2]^+$ 467.0543, found 467.0545. Anal. Calcd for $C_{12}H_{21}O_{14}PNa_2\cdot 2H_2O$: C, 28.70; H, 5.02. Found: C, 28.61; H, 5.21.

Enzyme Kinetics

All kinetic assays were conducted in 1 cm path length matched quartz cuvettes with a Cary 300 UV−vis spectrometer equipped with a circulating water bath, or a Cary 4000 UV−vis spectrometer with a Cary temperature controller attached. Unless stated otherwise, BglT was preincubated in the assay buffer at 50 °C for 5 min prior to the addition of substrate to initiate the enzymatic reaction. All data fitting was performed with GraFit version 4.0 or Cary WinUV, Kinetics Application, version 3.00 (182).

The following buffer systems were employed: buffer A, 50 mM HEPES, 0.1 mM $MnCl_2$, 1 μM NAD^+, 10 mM 2-mercaptoethanol, and 0.1% (w/v) BSA at pH 7.5; buffer B (all reagents were lyophilized twice from 99.9% D_2O), 50 mM HEPES, 0.1 mM $MnCl_2$, 1 μM NAD^+, 10 mM 2-mercaptoethanol (d_6), and 0.1% (w/v) BSA at pD 8.1.

Conditions for Measurement of Initial Rates. The concentration of BglT used for each substrate was chosen such that less than 10% of the total substrate was consumed, ensuring linear rates. BglT was preincubated with the assay buffer mixture for 5 min, and the reaction was initiated by the addition of the appropriate substrate. The initial rate of hydrolysis was followed spectrophotometrically upon addition of the appropriate aryl 6-phospho-β-D-glucoside at the wavelength of maximal absorbance difference between the released phenol and the respective aryl 6-phospho-β-D-glucoside.

Conditions for the Substrate Depletion Method (28). The k_{cat}/K_M analyses were performed by the depletion method using low substrate concentrations and by monitoring the change in absorbance at the wavelength of maximal absorbance difference between the released phenol and the respective aryl 6-phospho-β-D-glucoside over approximately 30 min until the reaction was complete. The data sets were fit to a first-order equation, and the k_{cat}/K_M values were obtained by dividing the pseudo-first-order rate constant that was obtained by the enzyme concentration.

Standard Procedures for Preparing Buffers and Enzyme in D_2O Solutions. All buffers and chemicals were lyophilized twice from 99.9% D_2O. Prior to kinetic assays, BglT was exchanged into deuterated buffer solutions via repeated (three times) dilution and concentration using a centrifugal filter unit (Millipore) with a nominal molecular weight limit (NMWL) of 10 000.

Kinetic Isotope Effect Measurements for 1[^{2}H]4NPG6P

The measurement of initial rates in buffer A for the hydrolysis of 4NPG6P and 1[^{2}H]4NPG6P allowed the determination of $(k_{cat})_H/(k_{cat})_D$. The final substrate (4NPG6P or 1[^{2}H]4NPG6P) concentration was 615 μM (>10K_M), and the final concentration of BglT was 4.5 μg/mL in an assay volume of 1 mL. Initial rates of hydrolysis were measured in alternation for substrates, 4NPG6P or 1[^{2}H]4NPG6P, 10 times each, and KIEs $[(k_{cat})_H/(k_{cat})_D]$ were calculated from the data, by dividing the rate for the protio substrate by the rate for the deuterio substrate in each case.

For $(k_{cat}/K_M)_H/(k_{cat}/K_M)_D$ measurements, the substrate depletion method was applied. BglT (final concentration of 9.0 μg/mL) was incubated in buffer A, and 4NPG6P or 1[^{2}H]-4NPG6P [final concentration of 6.15 μM (=0.15K_M), total assay volume of 1 mL] was used to initiate the enzymatic reaction. Each measurement was repeated 10 times in alternation, and the $(k_{cat}/K_M)_H/(k_{cat}/K_M)_D$ value was calculated by dividing the first-order rate constant for the protio substrate by the first-order rate constant for the deuterio substrate in each case.

pD Dependence

BglT and all reagents were exchanged into D_2O buffer. BglT was incubated at a series of pD values, and aliquots were periodically removed for assay at pD 7.5. These studies revealed that BglT was stable in the range pD 4.0−10.0. The pD dependence of k_{cat}/K_M was then determined by measurement of k_{cat}/K_M at a series of pD values using the substrate depletion method. All experiments were carried out at 50 °C in 50 mM NaCl, 0.1 mM $MnCl_2$, 1 μM NAD^+, 10 mM 2-mercaptoethanol (d_6), and 0.1% (w/v) BSA containing

either 20 mM AcOD/NaOAc (pD 4.0−4.5), 20 mM MES (pD 6.1−6.7), 20 mM HEPES (pD 6.5−8.2), or 20 mM CHES (pD 8.4−9.4). The enzyme (final concentration of 20.7 or 5.2 μg/mL) was preincubated with the solutions described above (final assay volume of 200 μL) at 50 °C for 5 min, and 4NPG6P [final concentration of 5.85 μM (=0.08K_M)] was used to initiate the enzymatic reaction. The k_{cat}/K_M values were obtained by dividing the pseudo-first-order rate constant by the enzyme concentration. The pD dependence of k_{cat}/K_M was fit to an equation describing a reaction governed by two essential ionizations.

Solvent Deuterium Kinetic Isotope Effect

Buffers, chemicals, and the enzyme stock solution were prepared in D_2O. The enzyme (final concentration of 1.03 μg/mL) was preincubated in buffer B, and initial rates were measured upon addition of 4NPG6P to a final assay volume of 200 μL. The assay pD was chosen to be 8.1, at which the rate is optimal and independent of pD. The difference in extinction coefficients, $\Delta\epsilon$, between 4NPG6P and the 4-nitrophenolate anion at pD 8.1 and 50 °C was determined to be 12 612 M^{-1} cm^{-1}, and the catalytic parameters were determined on the basis of a direct fit of the data to the Michaelis−Menten equation.

Primary Kinetic Isotope Effect Measurements for 2[^{2}H]4NPG6P in D_2O Buffer

Buffers, chemicals, and the enzyme stock solution were prepared in D_2O. All experiments were carried out in buffer B (final assay volume of 1 mL). For $(k_{cat})_H/(k_{cat})_D$ measurements, initial rates were measured for 2[^{2}H]4NPG6P or 4NPG6P using BglT (final concentration of 4.1 μg/mL), at a final substrate concentration of 580 μM (>8K_M). With alternation between the protio and deuterio substrates, linear initial rates were measured for 4NPG6P and 2[^{2}H]4NPG6P, and the KIE $(k_{cat})_H/(k_{cat})_D$ was calculated by dividing the rate constant for the protio substrate by the rate constant for the deuterio substrate. The set of experiments was repeated 10 times, and the average KIE value was calculated from the data.

Measurement of $(k_{cat}/K_M)_H/(k_{cat}/K_M)_D$ was performed using the substrate depletion method in which BglT (final concentration of 8.2 μg/mL) was preincubated in buffer B (final assay volume of 1 mL), with 4NPG6P or 2[^{2}H]4NPG6P [final concentration of 5.85 μM (=0.08K_M)] alternately. The resulting data set was fit to a first-order curve, and the k_{cat}/K_M values were obtained by dividing the pseudo-first-order rate constant by the enzyme concentration. The set of experiments was repeated nine times, and the average $(k_{cat}/K_M)_H/(k_{cat}/K_M)_D$ value was calculated from the data by dividing the first-order rate constant for the protio substrate by the first-order rate constant for the deuterio substrate in each case.

Determination of the K_d Value for NAD$^+$

BglT (1 mL, 1 mg/mL) was first dialyzed against 5 × 3 L of 50 mM HEPES at pH 7.5 to remove any bound NAD^+ prior to manipulation. Samples of dialyzed BglT (final concentration of 2.25 μg/mL) and NAD^+ (concentration varied from 100 nM to 10 μM) were preincubated in 50 mM HEPES, 0.1 mM $MnCl_2$, 10 mM 2-mercaptoethanol, and 0.1% (w/v) BSA at pH 7.5 for 5 min; then 4NPG6P [final concentration of 615 μM (>10K_M)] was added to the reaction mixture to give a final volume of 200 μL, and initial rates were measured. The reaction rate was plotted against the concentration of NAD^+ to generate a ligand binding curve.

Kinetic and Spectroscopic Investigation of Cofactor Reduction

For the kinetic analysis, a sample of dialyzed BglT [final concentration of 2.25 μg/mL (47 nM)] and NAD^+ (final concentration of 10 μM) was preincubated in buffer A for 5 min, and then 4NPG6P was added to the reaction mixture (final volume of 200 μL) to a final concentration of 615 μM (>10K_M). In a second reaction, dialyzed BglT [final concentration of 2.25 μg/mL (47 nM)], NAD^+ (final concentration of 10 μM), and $NaBH_4$ (final concentration of 10 mM) was preincubated in buffer A for 5 min, and 4NPG6P (final concentration of 615 μM) was added to a final assay volume of 200 μL. The change in A_{400} was monitored for 18 min prior to the addition of 10 μL of 200 μM NAD^+ to rescue enzyme activity. The change in A_{400} was then measured for an additional 20 min.

The absorbance spectra (from 250 to 400 nm) of the following three dialyzed enzyme samples were measured in 1 mL, 1 cm path length matched quartz cuvettes: 10 μM BglT, 10 μM BglT incubated with 10 μM NAD^+, and 10 μM BglT incubated with 10 μM NAD^+ and 10 mM sodium borohydride. Measurement of the sample pH after reaction confirmed that 10 mM sodium borohydride did not significantly alter the pH of the solution.

Glucose-6-phosphate Dehydrogenase Coupled Assay

C6′P was synthesized as described by Thompson and coworkers (*24*). Reaction rates were measured using a glucose-6-phosphate dehydrogenase (G6PDH) coupled assay. All experiments were carried out at 50 °C in buffer A, and 2 mM $NADP^+$ and 20 units of G6PDH. The activity of BglT was measured spectrophotometrically by monitoring the formation of the NADPH cofactor at 340 nm. Initial rates were measured upon addition of C6′P to the reaction mixture (final volume of 200 μL), by monitoring the increase in absorbance at 340 nm. Eight to twelve data points were collected for C6′P (final substrate concentration range of 10−1600 μM, final enzyme concentration of 5.63 μg/mL). The molar extinction coefficient of 6220 M^{-1} cm^{-1} ($\Delta\epsilon$ of NADPH) was used for the calculation of initial rates of substrate hydrolysis, and the catalytic parameters were determined on the basis of a direct fit of the data to the Michaelis−Menten equation. The concentration of BglT was doubled for two data points, and the observed rate was also doubled, ensuring that concentrations of G6PDH and $NADP^+$ used for the coupled assay were not the rate-limiting factors. Furthermore, BglT was assayed with 4NPG6P in the presence of 2 mM $NADP^+$, and the enzyme was also assayed with 4NPG6P in the presence of 20 units of G6PDH. In each case, the observed rate was the same as that when BglT was assayed alone, indicating that the presence of $NADP^+$ and G6PDH did not affect the activity of BglT.

Brønsted Analysis

Each aryl 6-phospho-β-D-glucoside was assayed in buffer A, and initial rates were measured. The typical substrate

Table 1: Michaelis−Menten Kinetic Parameters for the Hydrolysis of a Series of Aryl 6-Phospho-β-D-glucosides by BglT at 50 °C and pH 7.5

aryl 6-phospho-β-D-glucoside	phenol pK_a	k_{cat} (s^{-1})	K_M (μM)	k_{cat}/K_M (s^{-1} mM^{-1})	$\Delta\epsilon$ (M^{-1} cm^{-1})	λ_{max} (nm)
24DNPG6P	3.96	2.29	44.4	52	10282	400
25DNPG6P	5.15	1.95	16.6	117	4383	443
34DNPG6P	5.36	1.15	31.4	37	15982	400
4Cl2NPG6P	6.45	1.69	15.0	113	4164	428
4NPG6P	7.18	0.99	48.6	20	13791	400
2NPG6P	7.22	1.21	17.4	70	3719	413
35DCG6P	8.19	2.33	41.4	56	1799	285
3NPG6P	8.39	4.69	72.9	64	312	380
4CNPG6P	8.49	1.01	45.4	22	8101	272
PG6P	9.99	0.79	31.9	25	1850	270
4tBuPG6P	10.37	1.21	58.3	21	1156	276

concentrations range from $0.7K_M$ to $7K_M$, and 7−10 data points were collected for each substrate. The concentration of BglT used in the final assay volume of 200 μL varied from 2.25 to 4.5 μg/mL. The difference in extinction coefficients ($\Delta\epsilon$) between the aryl 6-phospho-β-D-glucoside and the phenol released at pH 7.5 and 50 °C was determined by the method described by Kempton and Withers (*29*). The catalytic parameters (k_{cat} and K_M) were determined on the basis of a direct fit of the data to the Michaelis−Menten equation. The data are presented in Table 1. Logarithms of the k_{cat} and k_{cat}/K_M values were plotted against the leaving group pK_a values. The Brønsted coefficient was obtained from the slope of this plot.

RESULTS

Determination of the K_d Value for NAD$^+$. BglT was assayed in the presence of various concentrations of NAD^+, the enzyme being completely inactive in the absence of NAD^+. As shown in Figure 2, the data were fit to a simple hyperbolic binding equation, and a K_d value of 480 nM for the binding of the dinucleotide cofactor to BglT was determined.

Kinetic and Spectroscopic Investigation of Cofactor Reduction. The absorbance spectra (from 320 to 400 nm) of BglT were recorded under three differing conditions: 10 μM BlgT, 10 μM BglT incubated with 10 μM NAD^+, and 10 μM BglT incubated with 10 μM NAD^+ and 10 mM sodium borohydride (Figure 3). The peak in absorbance at 340 nm corresponding to NADH appears upon reduction with 10 mM sodium borohydride, and is consistent with the quantitative reduction of NAD^+ to NADH. On the basis of the small K_d value of 480 nM for NAD^+, more than 99% of BglT has NAD^+ or NADH bound to its active site under these conditions, and very little remains free in solution. BglT activity was assayed in the presence of NAD^+, and the activity was compared to that obtained in the presence of NADH (quantitatively reduced from NAD^+ using sodium borohydride) as shown in Figure 4. The enzyme was completely inactive in the presence of NADH (reduced form) alone. Upon addition of excess NAD^+, full activity (Figure 4) was rapidly restored, demonstrating that the loss of activity upon reduction is due solely to having the dinucleotide cofactor in the wrong redox state rather than protein denaturation or dramatic changes in pH.

pD Dependence Measurements. The pD dependence of k_{cat}/K_M for BglT in H_2O and D_2O was determined by the substrate depletion method (*28*). Values of k_{cat}/K_M versus pD were fit to an equation describing the dependence of rate upon two essential ionizations, and the bell-shaped curve shown in Figure 5 was obtained. The pD dependence of k_{cat}/K_M was shown to have a pD optimum of 8.8, with two apparent pK_a values of 7.63 ± 0.06 and 9.90 ± 0.09. The pH dependence (in H_2O) had been shown previously to have a pH optimum of 8.0, with two apparent pK_a values of 7.08 ± 0.07 and 9.31 ± 0.08. The pD dependence of k_{cat}/K_M is plotted along with the pH dependence of k_{cat}/K_M in Figure 5 (*6*).

Solvent Kinetic Isotope Effect. A solvent KIE was measured for BglT using 4NPG6P at pD 8.1. This pD was selected because at this value rates are optimal in both H_2O and D_2O (see Figure 5). Michaelis−Menten kinetic behavior

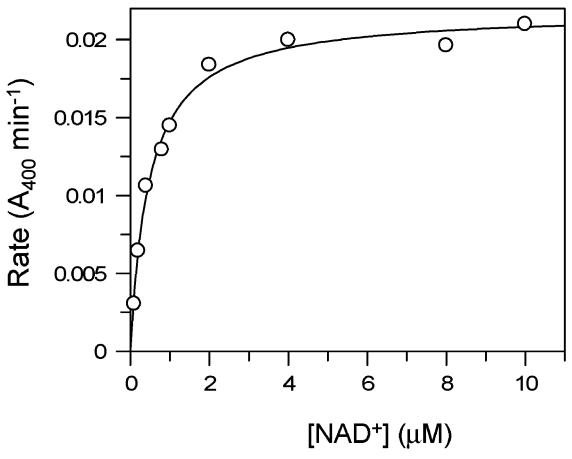

FIGURE 2: Ligand binding curve of NAD^+.

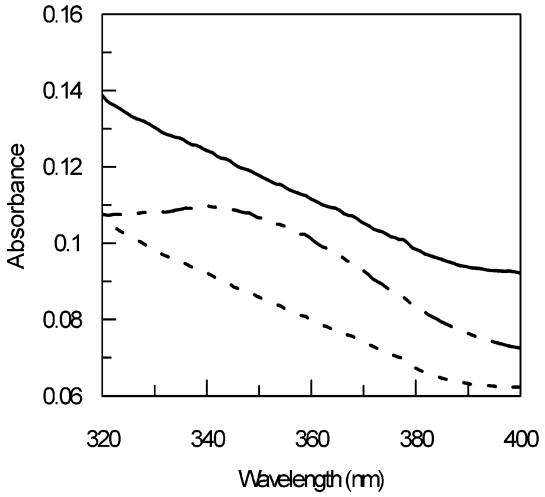

FIGURE 3: Absorbance spectra of 10 μM BlgT (—), 10 μM BglT incubated with 10 μM NAD^+ (- - -), and 10 μM BglT incubated with 10 μM NAD^+ and 10 mM sodium borohydride (— - —).

Table 2: Kinetic Isotope Effect Measurements for Deuterated Substrates of BglT

	$[(k_{cat})_H/(k_{cat})_D]_{H_2O}$	$[(k_{cat}/K_M)_H/(k_{cat}/K_M)_D]_{H_2O}$	$[(k_{cat})_H/(k_{cat})_D]_{D_2O}$	$[(k_{cat}/K_M)_H/(k_{cat}/K_M)_D]_{D_2O}$
1[^{2}H]4NPG6P	1.00 ± 0.01	1.01 ± 0.04	–	–
2[^{2}H]4NPG6P	1.84 ± 0.02[a]	2.03 ± 0.01[a]	1.62 ± 0.04	1.60 ± 0.09
3[^{2}H]4NPG6P	1.63 ± 0.01[a]	1.91 ± 0.03[a]	–	–

[a] Data obtained from ref *5*.

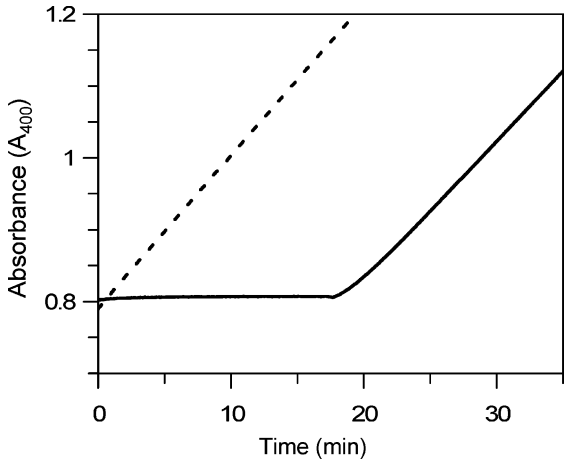

FIGURE 4: Assay of BglT in the oxidized (NAD^+) and reduced (NADH) state. Observed rates of hydrolysis of 4NPG6P by BglT via detection of 4-nitrophenolate release at 400 nm. Control (- - -): standard BglT assay conditions, 50 mM HEPES (pH 7.5), 0.1 mM $MnCl_2$, 10 μM NAD^+, 10 mM 2-mercaptoethanol, and 0.1% (w/v) BSA at 50 °C. BglT assay conditions (—): enzyme preincubated in 50 mM HEPES (pH 7.5), 0.1 mM $MnCl_2$, 10 μM NAD^+, 10 mM $NaBH_4$, 10 mM 2-mercaptoethanol, and 0.1% (w/v) BSA at 50 °C. No release of 4-nitrophenolate is observed until 18 min, when 2 nmol of NAD^+ was added.

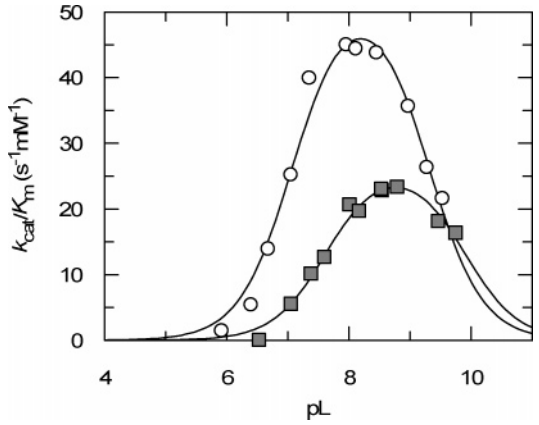

FIGURE 5: pL dependence of the k_{cat}/K_M for BglT. The empty circles represent the data obtained in H_2O previously (*6*), and the filled squares represent the data obtained in D_2O.

was observed, and the k_{cat} and K_M values at pD 8.1 in D_2O were found to be 0.72 s^{-1} and 70 μM, respectively; the values in H_2O were 0.91 s^{-1} and 40 μM, respectively. The solvent KIE values were therefore determined: $(k_{cat})_{H_2O}/(k_{cat})_{D_2O} = 1.3$ and $(k_{cat}/K_M)_{H_2O}/(k_{cat}/K_M)_{D_2O} = 2.2$.

Kinetic Isotope Effect for 2[^{2}H]4NPG6P Measured in D_2O. The deuterium KIE associated with the 2-position was measured in D_2O buffer using 4NPG6P and 2[^{2}H]4NPG6P. The $[(k_{cat})_H/(k_{cat})_D]_{D_2O}$ value measured at a substrate concentration of 8 K_M was found to be 1.62 ± 0.04. The $[(k_{cat}/K_M)_H/(k_{cat}/K_M)_D]_{D_2O}$ value was determined to be 1.60 ± 0.09, measured at a substrate concentration equal to 0.08K_M. Small yet significant primary KIE values are therefore observed in D_2O buffer, much as was previously measured in H_2O buffer: $[(k_{cat})_H/(k_{cat})_D]_{H_2O} = 1.84 \pm 0.02$ and $[(k_{cat}/K_M)_H/(k_{cat}/K_M)_D]_{H_2O} = 2.03 \pm 0.01$ (*5*).

Kinetic Isotope Effect for 1[^{2}H]4NPG6P Measured in H_2O. α-Deuterium kinetic isotope effects for cleavage of 1[^{2}H]-4NPG6P were measured at two different substrate concentrations to give isotope effects on k_{cat} and on k_{cat}/K_M. The $(k_{cat})_H/(k_{cat})_D$ value measured at a substrate concentration of 15K_M was found to be 1.00 ± 0.01, while the $(k_{cat}/K_M)_H/(k_{cat}/K_M)_D$ value was determined to be 1.01 ± 0.04 at a substrate concentration equal to 0.15K_M. The absence of any KIE upon $(k_{cat})_H/(k_{cat})_D$ or $(k_{cat}/K_M)_H/(k_{cat}/K_M)_D$ resulting from deuterium substitution at C1 indicates that rehybridization at C1 is not occurring at the rate-limiting transition state and probably that the cleavage of the C1−O1 linkage is not rate-determining. All KIE data are summarized in Table 2.

Glucose-6-phosphate Dehydrogenase Coupled Assay. A coupled assay involving BglT and G6PDH was utilized to determine the kinetic parameters for the natural substrate C6′P. The C6′P substrate displayed Michaelis−Menten kinetics, with the following kinetic parameters: $k_{cat} = 0.61$ s^{-1} and $K_M = 69$ μM.

Linear Free Energy Relationship: Brønsted Analysis. To determine whether cleavage of the glycosidic bond is itself rate-limiting, a full Brønsted analysis was performed using a series of aryl 6-phospho-β-D-glucosides with phenol leaving groups of varying reactivity. 24DNPG6P, 25DNPG6P, 34DNPG6P, 4Cl2NPG6P, 4NPG6P, 2NPG6P, 35DCPG6P, 3NPG6P, 4CNPG6P, PG6P, and 4tBuPG6P were prepared (see Materials and Methods). The pK_a values of the leaving group phenols range from 3.96 to 10.37. Values of k_{cat} and K_M were determined for each substrate, and the values are presented in Table 1 along with their respective phenol pK_a values. The logarithms of k_{cat} and k_{cat}/K_M were calculated, and each was plotted against the pK_a of the leaving group. The Brønsted plots thereby produced are shown in Figure 6. Neither k_{cat} nor k_{cat}/K_M is significantly dependent on the phenol leaving group ability for these aryl 6-phospho-β-D-glucosides.

DISCUSSION

A central feature of the mechanism proposed for BglT is the bound NAD^+ cofactor and its role in transient redox chemistry. Such essential "on-board" NAD^+ cofactors have been seen and characterized in a number of other enzymes, wherein they carry out a transient oxidation to acidify an adjacent proton or to permit epimerization via reduction from the opposite face. Such enzymes include epimerases (*30*), decarboxylases (*23*), and dehydratases (*21*, *22*). Analysis of the three-dimensional structure of BglT reveals that the NAD^+ is perfectly positioned under the C3 hydrogen atom of the substrate for hydride abstraction, and thus oxidation, at that center. In addition, the measurement of a primary deuterium kinetic isotope effect at C3 and the observation

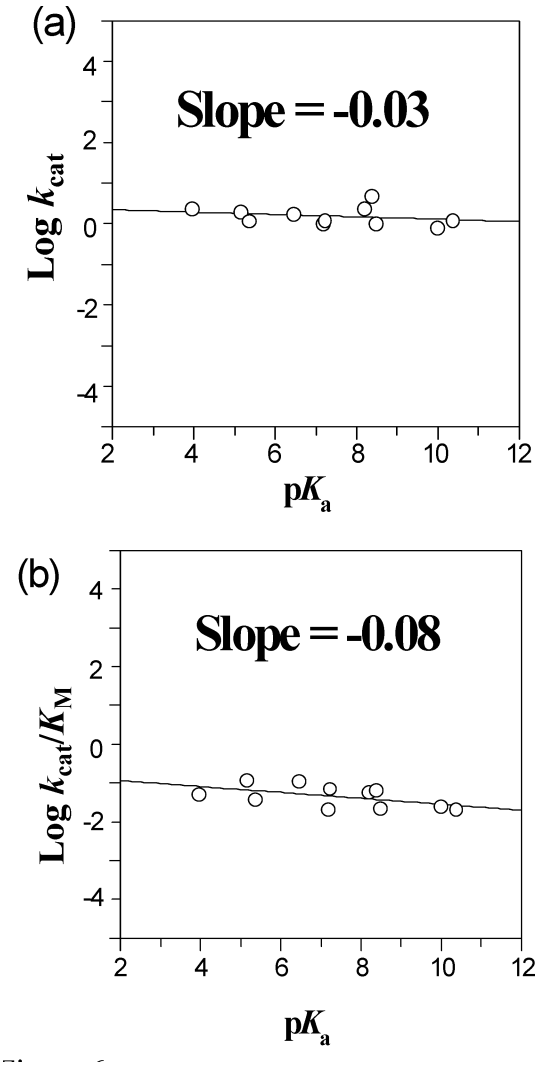

FIGURE 6: Brønsted plots of the enzymatic cleavage of a series of aryl 6-phospho-β-D-glucosides with the corresponding pK_a values for the leaving group phenol: (a) log k_{cat} vs pK_a and (b) log k_{cat}/K_M vs pK_a.

of solvent deuterium exchange at H2 had provided evidence of an oxidation at C3 during catalysis (*5*). However, no direct evidence for the involvement of NAD^+ in redox chemistry during catalysis had been generated (*13*, *15*, *19*). Further, some confusion exists in the literature concerning the possibility that NADH, as well as NAD^+, could activate the enzymes in this family (*15*, *20*). These items therefore merited closer analysis.

The observation that dialysis of NAD^+ from the enzyme removed all catalytic activity and that full activity could be restored in a saturable fashion by titration with NAD^+ supported an essential role for NAD^+ and yielded a dissociation constant (K_d) for NAD^+ of 480 nM. Further support for this, and direct proof that the reduced form (NADH) was inactive, was derived by reduction of an enzyme sample with sodium borohydride and demonstration that this enzyme form was devoid of activity. Analysis of these samples by UV−visible spectrophotometry confirmed that the bound NAD^+ had indeed been reduced to NADH (λ_{max} = 340 nm). Importantly, addition of a fresh aliquot of NAD^+ to this sample (after sufficient time had elapsed for consumption of excess $NaBH_4$) restored the enzyme to full activity. This confirmed the essential role of NAD^+ and showed that loss of activity was not caused by other damage to the enzyme. It also confirmed that NADH could not activate the enzyme, consistent with the mechanism. The activation observed previously arose presumably from contaminating NAD^+ within the NADH sample (*15*, *20*). Very little would be needed given the low K_d for NAD^+ and the catalytic amounts of enzyme employed in those experiments.

The measurement of small but significant primary kinetic isotope effects on the hydrolysis of 3[^{2}H]4NPG6P and 2[^{2}H]-4NPG6P provided evidence both for the oxidation at C3 and for the proton abstraction at C2, as well as suggesting that both steps were partially rate-limiting (*5*). However, the possibility remained that the true deuterium kinetic isotope effect at the 2-position was much larger, but that its value had been suppressed by exchange of the C2 deuterium for solvent H_2O during the measurement. This would be a significant concern if the reprotonation of the anion generated at C2 occurs at a greater rate than that of the elimination step. As a first test of this possibility, samples of unreacted residual 4NPG6P incubated with BglT in D_2O buffer were analyzed by mass spectrometry, and no incorporation of deuterium was observed. While this suggests that no exchange occurs, it is not conclusive since the observation of exchange would require that the reduction at C3 also occur more rapidly than elimination, which is not necessarily the case. Measurement of the kinetic isotope effect for 2[^{2}H]-4NPG6P in D_2O should provide a more stringent test since any exchange in that case would leave deuterium in place, and the full KIE should be observed. However, it was first necessary to establish whether the overall reaction exhibited any significant solvent deuterium kinetic isotope effect and to determine whether ionizations in the enzyme, thus possibly the pH optima, are significantly different in D_2O buffer versus H_2O buffer. The results in Figure 5 clearly show a shift in the acidic limb of the pH profile, with a much smaller shift in the pH optimum. Such a shift of approximately 0.6 unit in the two apparent pK_a values is consistent with the typical solvent isotope effects observed for the ionization of a number of general acids (*31*). However, the activity is essentially maximal at pL 8.1 in both cases, thereby ensuring that kinetic isotope effect measurements at this pH will be meaningful. Redetermination of deuterium kinetic isotope effects on k_{cat} and k_{cat}/K_M for 2[^{2}H]4NPG6P in D_2O revealed only small differences from those measured in H_2O (Table 2). Therefore, these isotope effects are indeed small, and no significant reprotonation of the anion occurs during catalysis; elimination occurs more rapidly. Such a small kinetic isotope effect is indeed consistent with the cleavage of the C2−H2 bond only being partially rate-limiting.

The results described above suggest that the actual glycosidic bond cleavage step, the elimination, is likely to be relatively rapid in comparison to the hydride and proton abstraction steps. This notion was probed in two ways, through Brønsted analysis and through the measurement of an α-deuterium kinetic isotope effect on 1[^{2}H]4NPG6P. The results shown in Figure 6 clearly show the lack of any significant dependence of the rate constant k_{cat} or k_{cat}/K_M upon aglycon leaving group ability. The simplest, and most likely, interpretation is that this elimination step is relatively fast and not rate-limiting. However, the possibility remains that the step could be rate-limiting, but that there is no significant buildup of negative charge on the phenolate oxygen at the

Scheme 1: Enzymatic Reactions in the G6PDH Coupled Assay for the Natural Substrate C6′P

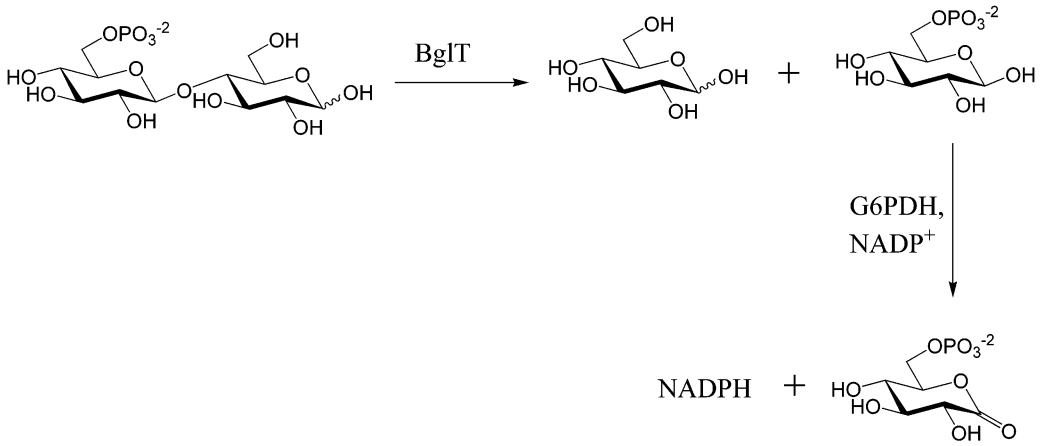

rate-limiting transition state due to efficient proton donation. The absence of a significant α-deuterium kinetic isotope effect on hydrolysis of 1[^{2}H]4NPG6P demonstrated that this latter scenario was not the case. If bond cleavage had been rate-limiting, then that step would be associated with significant rehybridization at the anomeric center as the anionic carbon becomes sp^2-hybridized. Since no significant KIE was observed, it is concluded that this elimination step is relatively fast and therefore kinetically silent.

All the experiments described to date were performed on artificial aryl glycoside substrates, and thus provide insight into the mechanism of cleavage of activated glycoside substrates. Conclusions that have been drawn are certainly relevant for those substrates and provide valuable insights into how the enzyme functions. Indeed, all steps following aglycon elimination are common. However, they may be misleading if these artificial substrates are cleaved at vastly different rates than are the natural substrates. To address this concern, it was necessary to measure kinetic parameters for the presumed natural substrate C6′P. This was achieved using the coupled assay depicted in Scheme 1, in which the glucose 6-phosphate that was liberated was converted to 6-phosphoglucono lactone by added G6PDH, with concomitant reduction of $NADP^+$, which can be monitored spectrophotometrically at 340 nm. Fortunately, there is no conflict in the use of this assay with the requirement of BglT for NAD^+, since BglT does not accept $NADP^+$ (*5*), and in any case, both enzymes require the same cofactor redox form; measurement of only initial rate kinetics ensures no significant buildup of the reduced form. Reassuringly, the kinetic parameters measured for C6′P ($k_{cat} = 0.61\ s^{-1}$, $K_M = 69\ \mu M$) are very similar to those for 4NPG6P ($k_{cat} = 0.99\ s^{-1}$, $K_M = 48\ \mu M$); thus, concerns of completely different mechanisms in the two cases seem unfounded.

In summary, the results presented here support and extend the proposed mechanism for BglT and, by extension, family 4 enzymes in general. The on-board NAD^+ effects a transient, and partially rate-limiting, oxidation of the substrate at C3, thereby acidifying the C2 proton. Partially rate-limiting proton abstraction follows, generating a metal-stabilized enediolate which rapidly undergoes elimination to generate the bound α,β-unsaturated ketone intermediate. The reaction is completed by addition of water to the Michael acceptor and reduction of the ketone by the on-board NADH. Thus, the enzyme employs a fully stepwise $E1_{cb}$ mechanism, involving anionic transition states, in stark contrast to all other currently characterized glycosidase families, which effect hydrolysis through cationic, oxocarbenium ion-like transition states.

ACKNOWLEDGMENT

We thank our collaborators Dr. G. J. Davies and Dr. A. Varrot for structural analyses and provision of the plasmid for BglT and Dr. J. Thompson for his kind donation of the kinase, BglK.

REFERENCES

1. Henrissat, B., and Bairoch, A. (1996) Updating the sequence-based classification of glycosyl hydrolases, *Biochem. J. 316*, 695−696.
2. Henrissat, B., and Davies, G. (1997) Structural and sequence-based classification of glycoside hydrolases, *Curr. Opin. Struct. Biol. 7*, 637−644.
3. Henrissat, B., Callebaut, I., Fabrega, S., Lehn, P., Mornon, J. P., and Davies, G. (1995) Conserved catalytic machinery and the prediction of a common fold for several families of glycosyl hydrolases, *Proc. Natl. Acad. Sci. U.S.A. 92*, 7090−7094.
4. Rajan, S. S., Yang, X., Collart, F., Yip, V. L. Y., Withers, S. G., Varrot, A., Thompson, J., Davies, G. J., and Anderson, W. F. (2004) Novel catalytic mechanism of glycoside hydrolysis based on the structure of an NAD^+/Mn^{2+}-dependent phospho-α-glucosidase from *Bacillus subtilis*, *Structure 12*, 1619−1629.
5. Yip, V. L. Y., Varrot, A., Davies, G. J., Rajan, S. S., Yang, X. J., Thompson, J., Anderson, W. F., and Withers, S. G. (2004) An unusual mechanism of glycoside hydrolysis involving redox and elimination steps by a family 4 β-glycosidase from *Thermotoga maritima*, *J. Am. Chem. Soc. 126*, 8354−8355.
6. Varrot, A., Yip, V. L. Y., Li, Y., Rajan, S. S., Yang, X., Anderson, W. F., Thompson, J., Withers, S. G., and Davies, G. J. (2005) NAD^+ and metal-ion dependent hydrolysis by family 4 glycosidases: Structural insight into specificity for phospho-β-D-glucosides, *J. Mol. Biol. 346*, 423−435.
7. Sinnott, M. L. (1990) Catalytic mechanisms of enzymatic glycosyl transfer, *Chem. Rev. 90*, 1171−1202.
8. Zechel, D. L., and Withers, S. G. (2000) Glycosidase mechanisms: Anatomy of a finely tuned catalyst, *Acc. Chem. Res. 33*, 11−18.
9. Vasella, A., Davies, G. J., and Böhm, M. (2002) Glycosidase mechanisms, *Curr. Opin. Chem. Biol. 6*, 619−629.
10. Rye, C. S., and Withers, S. G. (2000) Glycosidase mechanisms, *Curr. Opin. Chem. Biol. 4*, 573−580.
11. Koshland, D. E., Jr. (1953) Stereochemistry and the mechanism of enzymic reactions, *Biol. Rev. 28*, 416−436.
12. Bouma, C. L., Reizer, J., Reizer, A., Robrish, S. A., and Thompson, J. (1997) 6-Phospho-α-D-glucosidase from *Fusobacterium mortiferum*: Cloning, expression, and assignment to family 4 of the glycosylhydrolases, *J. Bacteriol. 179*, 4129−4137.
13. Raasch, C., Armbrecht, M., Streit, W., Höcker, B., Sträter, N., and Liebl, W. (2002) Identification of residues important for

NAD^+ binding by the *Thermotoga maritima* α-glucosidase AglA, a member of glycoside hydrolase family 4, *FEBS Lett. 517*, 267−271.
14. Thompson, J., Robrish, S. A., Immel, S., Lichtenthaler, F. W., Hall, B. G., and Pikis, A. (2001) Metabolism of sucrose and its five linkage-isomeric α-D-glucosyl-D-fructoses by *Klebsiella pneumoniae*: Participation and properties of sucrose-6-phosphate hydrolase and phosph-α-glucosidase, *J. Biol. Chem. 276*, 37415−37425.
15. Thompson, J., Pikis, A., Ruvinov, S. B., Henrissat, B., Yamamoto, H., and Sekiguchi, J. (1998) The gene *glvA* of *Bacillus subtilis* 168 encodes a metal-requiring, NAD(H)-dependent 6-phospho-α-glucosidase: Assignment to family 4 of the glycosylhydrolase superfamily, *J. Biol. Chem. 273*, 27347−27356.
16. Thompson, J., Gentry-weeks, C. R., Nguyen, N. Y., Folk, J. E., and Robrish, S. A. (1995) Purification from *Fusobacterium mortiferum* ATCC 25557 of a 6-phoshoryl-*O*-α-D-glucopyranosyl: 6-phosphoglucohydrolase that hydrolyzes maltose 6-phosphate and related phosho-α-D-glucosides, *J. Bacteriol. 177*, 2505−2512.
17. Thompson, J., Ruvinov, S. B., Freedberg, D. I., and Hall, B. G. (1999) Cellobiose-6-phosphate hydrolase (CelF) of *Escherichia coli*: Characterization and assignment to the unusual family 4 of glycosylhydrolases, *J. Bacteriol. 181*, 7339−7345.
18. Lapidus, A., Galleron, N., Sorokin, A., and Ehrlich, S. D. (1997) Sequencing and functional annotation of the *Bacillus subtilis* genes in the 200 kb rrnB-dnaB region, *Microbiology 143*, 3431−3441.
19. Lodge, J. A., Maier, T., Liebl, W., Hoffmann, V., and Sträter, N. (2003) Crystral structure of *Thermotoga maritima* α-glucosidase AglA defines a new clan of NAD^+-dependent glycosidases, *J. Biol. Chem. 278*, 19151−19158.
20. Thompson, J., Hess, S., and Pikis, A. (2004) Genes *malh* and *pagl* of *Clostridium acetobutylicum* ATCC 824 encode NAD^+- and Mn^{2+}-dependent phospho-α-glucosidase(s), *J. Biol. Chem. 279*, 1553−1561.
21. Allard, S. T. M., Beis, K., Giraud, M. F., Hegeman, A. D., Gross, J. W., Wilmouth, R. C., Whitfield, C., Graninger, M., Messner, P., Allen, A. G., Maskell, D. J., and Naismith, J. H. (2002) Toward a structural understanding of the dehydratase mechanism, *Structure 10*, 81−92.
22. He, X., Thorson, J. S., and Liu, H. W. (1996) Probing the coenzyme and substrate binding events of CDP-D-glucose 4,6-dehydratase: Mechanistic implications, *Biochemistry 35*, 4721−4731.
23. Gatzeva-Topalova, P. Z., May, A. P., and Sousa, M. C. (2005) Structure and mechanism of ArnA: Conformational change implies ordered dehydrogenase mechanism in key enzyme for polymyxin resistance, *Structure 13*, 929−942.
24. Thompson, J., Lichtenthaler, F. W., Peters, S., and Pikis, A. (2002) β-Glucoside kinase (BglK) from *Klebsiella pneumoniae*: Purification, properties, and preparative synthesis of 6-phospho-β-D-glucosides, *J. Biol. Chem. 277*, 34310−34321.
25. Conchie, J., and Levvy, G. A. (1963) Aryl glycopyranosides by the Koenigs-Knorr method, *Methods Carbohydr. Chem. 2*, 335−337.
26. Ballardie, F., Capon, B., Sutherland, J. D. G., Cocker, D., and Sinnott, M. L. (1973) A simple general synthesis of 2,4-dinitrophenyl glycopyranosides, *J. Chem. Soc., Perkin Trans. 1*, 2418−2419.
27. Sinnott, M. L., and Souchard, I. J. L. (1973) Mechanism of action of β-galactosidase: Effect of aglycone nature and α-deuterium substitution on hydrolysis of aryl galactosides, *Biochem. J. 133*, 89−98.
28. Joshi, M. D., Sidhu, G., Pot, I., Brayer, G. D., Withers, S. G., and McIntosh, L. P. (2000) Hydrogen bonding and catalysis: A novel explanation for how a single amino acid substitution can change the pH optimum of a glycosidase, *J. Mol. Biol. 299*, 255−279.
29. Kempton, J. B., and Withers, S. G. (1992) Mechanism of *Agrobacterium* β-glucosidase: Kinetic studies, *Biochemistry 31*, 9961−9969.
30. Thoden, J. B., Frey, A. F., and Holden, H. M. (1996) Molecular structure of the NADH/UDP-glucose abortive complex of UDP-galactose 4-epimerase from *Escherichia coli*: Implications for the catalytic mechanism, *Biochemistry 35*, 5137−5144.
31. Schowen, K. B., and Schowen, R. L. (1982) Solvent isotope effects on enzyme systems, *Methods Enzymol. 87*, 551−606.
32. Nieman, C. E., Wong, A. W., He, S., Clarke, L., Hopwood, J. J., and Withers, S. G. (2003) Family 39 α-L-Iduronidases and β-D-Xylosidases React through Similar Glycosyl-Enzyme Intermediates: Identification of the Human Iduronidase Nucleophile, *Biochemistry 42*, 8054−8065

BI052054X